مجلة جامعة فزان العلمية
Fezzan University scientific Journal
journal@fezzanu.edu.ly

Effects of Vertical Serpentine Pipe on Liquid Film Characteristics

*Almabrok Abushanaf Almabrok[1] and Sana Ibrahim Mohamed[2]

[1]Petroleum Engineering Department, Sirte University, Sirte- Libya
[2]Chemical Engineering Department, Sirte University, Sirte- Libya

Abstract
This study investigates the dynamics of liquid film thickness in both downward and upward-flow pipes, influenced by various superficial air and water velocities. Data collected from sensors reveals distinct flow characteristics. High airflow combined with low water flow rates results in large disturbance waves at upper and mid-level probes, while smaller wavelengths and lower amplitudes are observed under different conditions. The stabilisation of the liquid film in the middle and lower regions is attributed to reduced bending effects. Unique frequency patterns emerge near bends, showing significant differences in power spectral density (PSD) compared to more distant locations. Furthermore, the examination of probability density function (PDF) data highlights the substantial influence of air and water superficial velocities on flow dynamics, with variations observed across all tested velocity ranges. These findings illustrate the complex interplay of flow parameters and liquid film behaviour in multiphase systems.

Keywords: film thickness, PSD, PDF, flow characteristics, bend impacts

تأثير الأنابيب الرأسية المتعرجة على خصائص غشاء السائل

*المبروك أبوشناف المبروك[1] وسناء إبراهيم محمد[2]

[1]قسم هندسة النفط، جامعة سرت، سرت، ليبيا

[2]قسم الهندسة الكيميائية، جامعة سرت، سرت، ليبيا

الملخص

تبحث هذه الدراسة في ديناميكيات سماكة غشاء السائل في الأنابيب ذات التدفق الهابط والصاعد، متأثرةً بسرعات الهواء والماء السطحية المختلفة. تُظهر البيانات المُجمعة من أجهزة الاستشعار خصائص تدفق مميزة. يؤدي تدفق الهواء المرتفع مع معدلات تدفق الماء المنخفضة إلى موجات اضطراب كبيرة عند قياسها بواسطة المجسات العليا والمتوسطة المستوي، بينما يلاحظ أطوال موجية أصغر وسعات أقل في ظروف مختلفة. يُعزى استقرار غشاء السائل في المناطق الوسطى والسفلى إلى انخفاض تأثيرات الانحناء. تظهر أنماط تردد فريدة قرب الانحناءات، مما يُظهر اختلافات كبيرة في كثافة طيف القدرة (PSD)مقارنةً بالمواقع الأبعد. علاوةً على ذلك، يُبرز فحص بيانات دالة كثافة الاحتمال (PDF) التأثير الكبير لسرعات الهواء والماء السطحية على ديناميكيات التدفق، مع ملاحظة اختلافات في جميع نطاقات السرعة المُختبرة. توضح هذه النتائج التفاعل المُعقد بين مُعاملات التدفق وسلوك غشاء السائل في الأنظمة متعددة الأطوار.

*Corresponding author:
E-mail: almabrok.abushanaf@su.edu.ly Received in 1 march 2025 - revised form 24 march 2025
Accepted 8 April 2025 - Publication date: 20 April 2025

الكلمات المفتاحية: سُمك الغشاء، كثافة طيف القدرة، دالة كثافة الاحتمال، خصائص التدفق، تأثيرات الانحناء

1 Introduction

Liquid film thickness is essential in various industrial processes, including petroleum extraction, heat exchange systems, and chemical reactors. Numerous experiments have measured liquid film thickness in serpentine piping using techniques such as laser-induced fluorescence (LIF), and high-speed imaging. Smith et al. (2010) utilized high-speed imaging to study the impact of Reynolds number, pipe curvature, and fluid characteristics on liquid film thickness. Wang et al. (2012) employed electrical capacitance tomography to visualize and quantify liquid film dynamics in vertical upward pipes for different flow rates and diameters. In their study, Smith et al. (2015) found that flow rate and channel geometry significantly influenced film thickness in serpentine microchannels. Chen et al. (2015) highlighted surface tension's critical role in liquid film behaviour by altering the surface characteristics and fluid types in their experiments. Choi et al. (2015) compared measurement techniques, including LIF and high-speed imaging, identifying advantages and limitations for liquid film measurement in upward pipes. Wang et al. (2016) focused on flow instabilities and identified key regimes impacting liquid film thickness in serpentine systems. Zhang et al. (2017) used gamma-ray densitometry to measure liquid film thickness in downward pipes and explored how flow rate, angle, and fluid properties affected dynamics. Lee et al. (2017) demonstrated that optimizing liquid film thickness could improve heat transfer efficiency in serpentine heat exchangers. Park et al. (2017) measured liquid film thickness using various techniques like electrical impedance tomography and discussed their applications. Smith et al. (2018) compared techniques like ultrasonic sensors and capacitance probes to evaluate measurement accuracy and reliability in different flow configurations. Lastly, Liu et al. (2019) investigated downward liquid film hydrodynamics using high-speed imaging and pressure measurements, providing insights into gas entrainment mechanisms and film stability.

2 Overview of the Serpent Rig

The Serpent rig's collecting system features components that form upward and downward lines, connected by fittings like 180° bends, as shown in Fig 1. It includes valves, devices, and pressure sensors. Water and ventilation tanks supply water to the rig via a pump, while two compressors connected through a T-shaped junction provide air. An automated system monitors and records all measurements in the process.

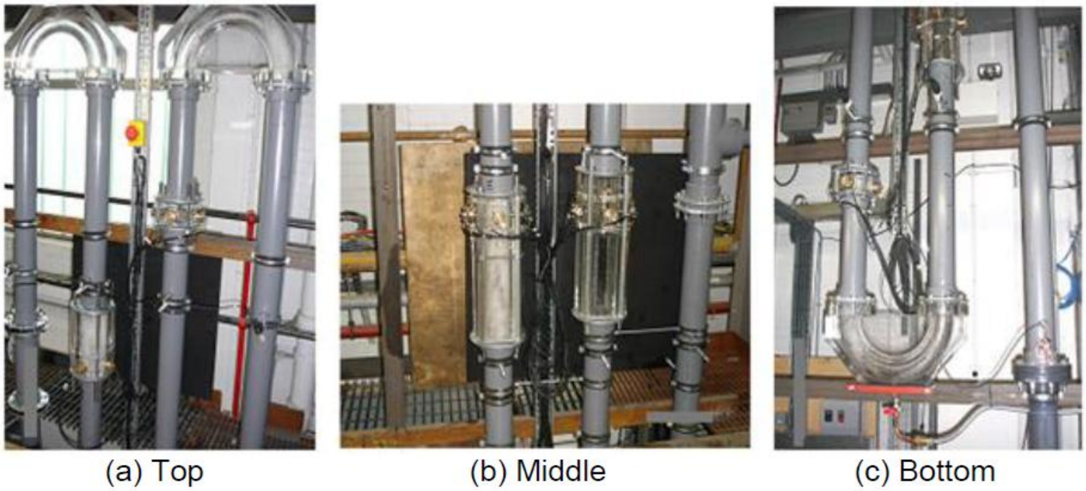

Figure 1 The test facility.

3 Results and discussion

The properties of the water film are evident in the profile of a time series & probability density function (PDF) for both downward and upward flows. In downflow, the film varies between the upper and lower regions because of the centrifugal effect from the upper curvature. This effect diminishes at mid-level and lower locations when liquid and gas flow rates are comparable. In upward flows, the PDF and time series indicate consistent film thickness across positions when velocities are equal. However, at lower flow, the film in upward flows was noticeably thicker than that in the opposite direction, suggesting that annular flow occurs only at high air superficial velocities. Additional experiments were conducted to establish annular flow in upward directions at higher flow rates. Overall, variations in the superficial velocities of air and water significantly impact the roughness of the air-water interface.

3.1 PDF, time profile & wave analysis in downflow orientation

The measurements presented in Fig. 2 were taken at three locations along the downflow path for liquid and gas velocities of 0.1 m/s & 3.02 m/s, respectively. The film's signal recorded at the higher region is significantly greater than those recorded at the mid-level and lower regions, which are similar. Large disturbance waves occur at the upper section due to the centrifugal force affecting the film thickness distribution there, while its effect is minor at the intermediate and lower positions. Sensor T2, aligned with the outer curvature of the bend, captures this influence. Furthermore, the wave patterns in the central and lower regions are more regular and coherent, indicating that the film reaches a stable state for the given gas and liquid flow velocities

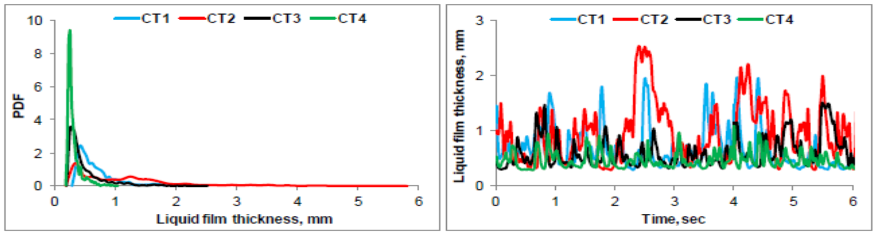

(a) Top position

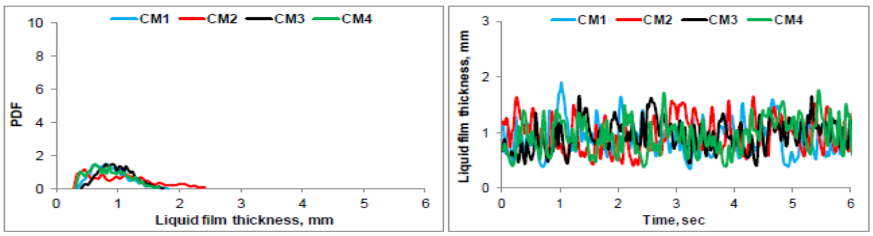

(b) Middle position

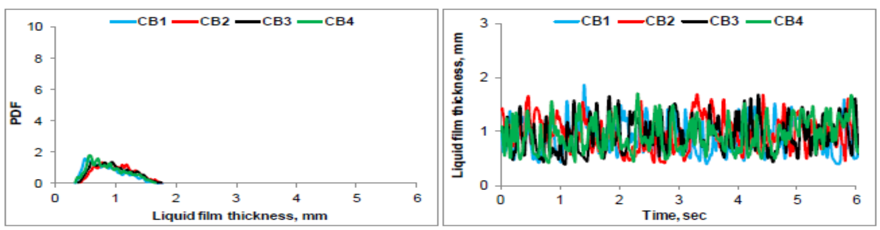

(c) Bottom position

Figure 2 time profile & PDF of the water film at three positions in a downward section: (a) upper, (b) middle, and (c) lower with water velocity= 0.1 m/s and gas velocity= 3.02 m/s.

The signals differ notably at the higher, mid-level, and lower regions, particularly from sensor T2 in the top probe, which is affected by centrifugal force (Fig. 3), where the velocities of water and gas are respectively 0.1 m/s and 28.87 m/s. At the higher region (Fig. 3a), the thickness of the liquid recorded by sensor T2 is significantly thicker when compared with the other films recorded by sensors T1, T3 & T4. The sensor M2 at a middle probe (Fig. 3b) shows greater thickness than sensors M1, M3, and M4. This indicates the bend's influence extends to the middle position but diminishes at the bottom position (46 pipe diameters away), where measurements from sensors B1, B2, B3, and B4 are similar. The profiles of the time at the bottom are more regular compared to the irregular waves at the top and middle. Sensors T2 and M2 display significant disturbance waves, while signals from T1, T3, and T4 have smaller wavelengths and amplitudes. The bend strongly influences the top and middle positions, but its effect weakens at the bottom. Additionally, T2 and M2 align with the outer radius of the bend, resulting in signals primarily influenced by the bend's effect.

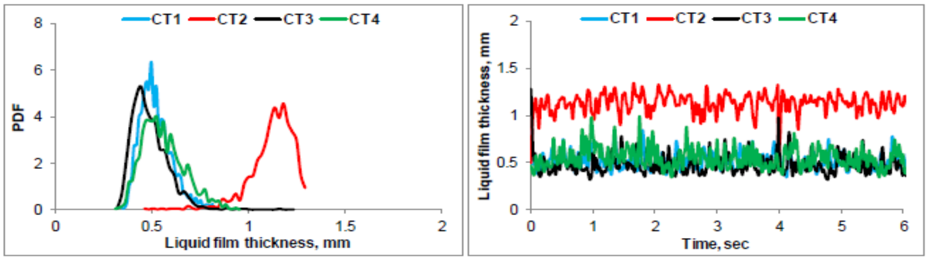

(a) Top position

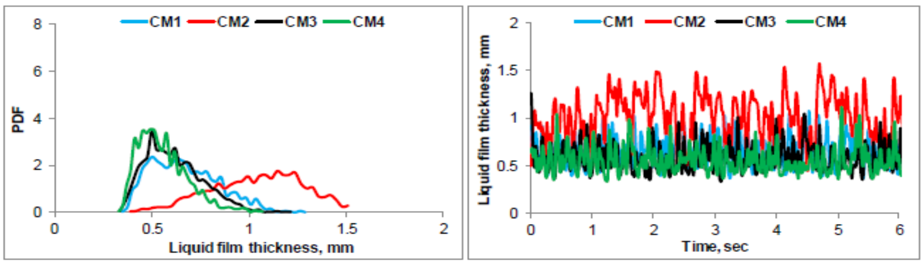

(b) Middle position

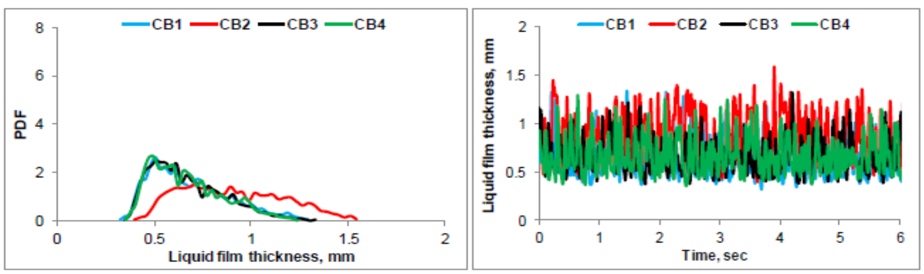

(c) Bottom position

Figure 3 time profile & PDF of the water film at three positions in a downward section: (a) upper, (b) middle, and (c) lower, with water velocity= 0.1 m/s and gas velocity= 28.87 m/s.

Figs 4 and 5 display the time profile and PDF of a water film in the downward flow at the top, mid-level, and lower regions, corresponding to a velocity of water (1 m/s) and air =2.67 m/s & 18.56 m/s. The film's signal from sensor T2 at the higher probe shows significant agitation and irregular waves with high peaks. This differs from the middle and bottom probes due to the force generated by the bend (centrifugal effect), affecting the film at sensor T2 aligned with a bend's outer curvature.

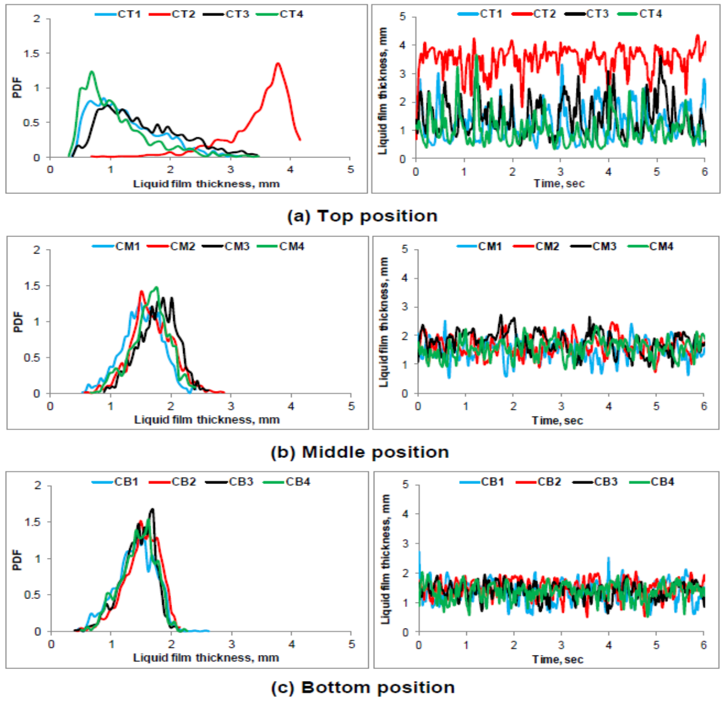

Figure 4 time profile & PDF of the water film at three positions in a downward section: (a) upper, (b) middle, and (c) lower, with water velocity= 1 m/s and gas velocity= 2.67 m/s.

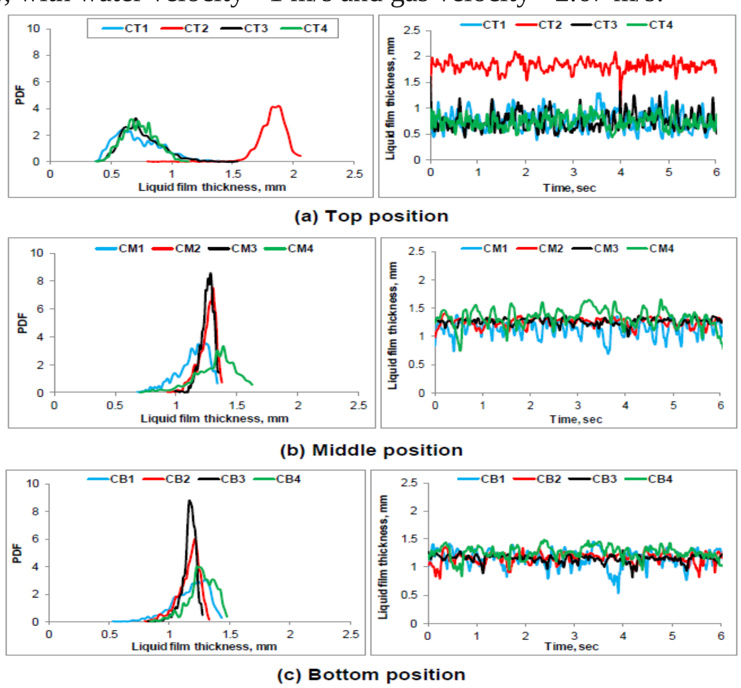

Figure 5 time profile & PDF of the water film at three positions in a downward section: (a) upper, (b) middle, and (c) lower, with water velocity= 1 m/s and gas velocity= 18.56 m/s.

3.2 Analysis of time profile, PDF, and wave behaviour of the water film in upflow

The time profile and PDF of the liquid film in the upward section were measured at various distances and different flow rates from the lower curvature, as shown in Figs 6 and 7. These measurements were taken at air superficial velocities of 3.02 m/s and 28.87 m/s, with a constant water superficial velocity of 0.1 m/s. At the gas velocity=3.02 m/s and liquid velocity=0.1 m/s, the PDF and the disturbance wave characteristics are similar across all positions, suggesting minimal variation in liquid film behaviour due to upstream centrifugal forces. Fig. 6 reveals significant disturbance waves at the higher, mid-level, and lower regions, contributing to intermittent flow behaviour. Fig. 7 shows that increasing gas flow rates, while maintaining a constant water flow rate, flattens these disturbance waves and results in thinner liquid films. This indicates that higher gas flow rates reduce liquid film thickness, as peak amplitudes in Fig. 7 appear lower than in Fig. 6.

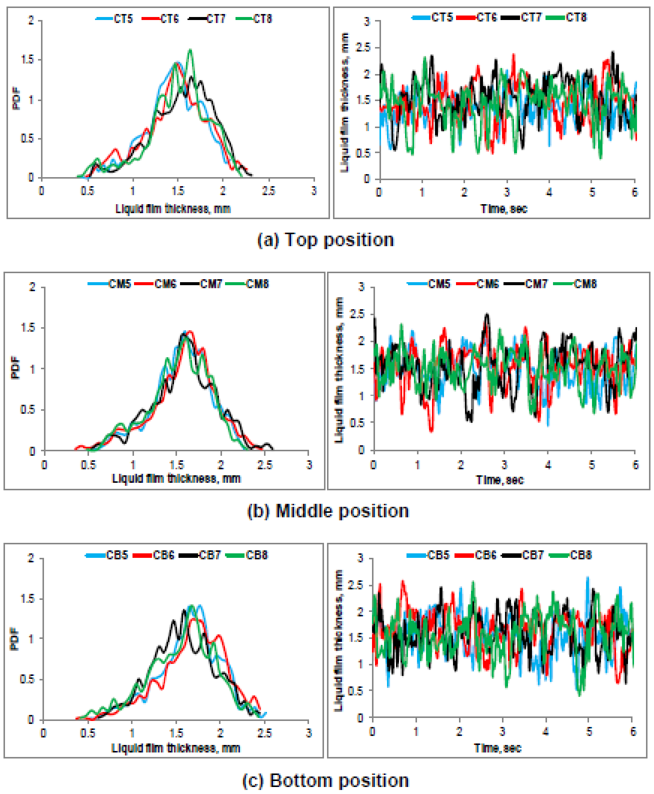

Figure 6 time profile and PDF of the water film at three positions in an upward section: (a) upper, (b) middle, and (c) lower, with water velocity= 0.1 m/s and gas velocity= 3.02 m/s.

The profile of water film recorded by the lower film device differs significantly from those recorded by the higher and mid-level devices. This difference explained in Fig. 7c, is due to the centrifugal forces acting on the bottom probe, affecting its film thickness measurements. Sensor B6 in the bottom probe measures a thicker film than sensors B5, B7, and B8, also shown in Fig. 7c. Additionally, the time traces indicate that the signal from B6 is slightly larger than those from the other sensors.

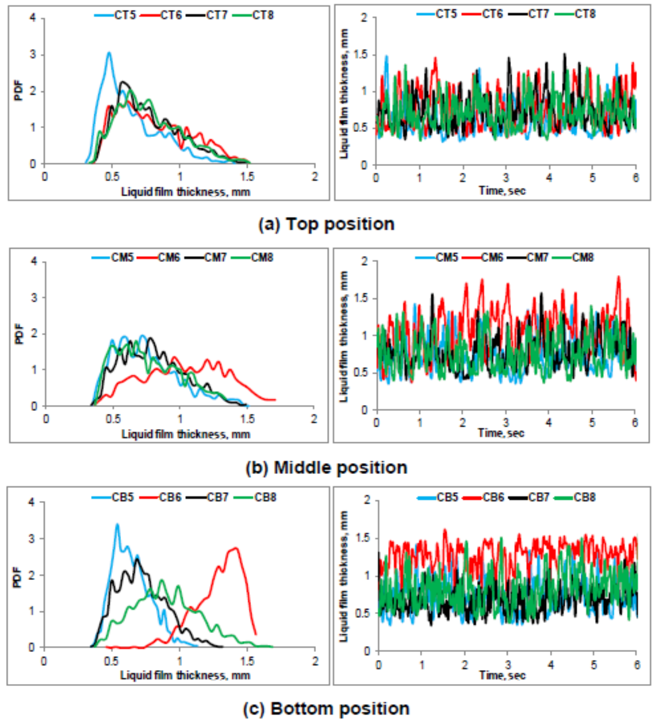

Figure 7 time profile & PDF of the water film at three positions in an upward section: (a) upper, (b) middle, and (c) lower, with water velocity= 0.1 m/s and gas velocity= 28.87 m/s.

Figs 8 and 9 illustrate the PDF and time profile of water film at three positions measured during upflow for a low velocity of gas phase=2.67 m/s & relatively high velocity=18.56 m/s, and for a constant velocity of water phase=1 m/s. The liquid film signal at the bottom region was noisier and exhibited a distinctly different PDF profile compared to the top and middle positions, varying circumferentially. This suggests that circumferential positioning may affect wave structure due to centrifugal forces at the bottom bend. Additionally, the amplitude of waves measured at the bottom region was significantly larger than those located in the upper regions, while the middle and top signals closely resemble each other. This indicates stabilization of the liquid film occurs beyond 28 pipe diameters, as supported by the similarity of waves observed at 28 and 47 pipe diameters. High-amplitude disturbance waves form continuously. In Figure 8c, disturbance waves exceed the probe's allowable range at the given superficial velocities, likely due to intermittent flow. When the velocity of gas increases to a higher value (i.e., to 18.56 m/s), annular flow develops, as shown in Fig. 9, resulting in lower peaks of disturbance waves across all positions.

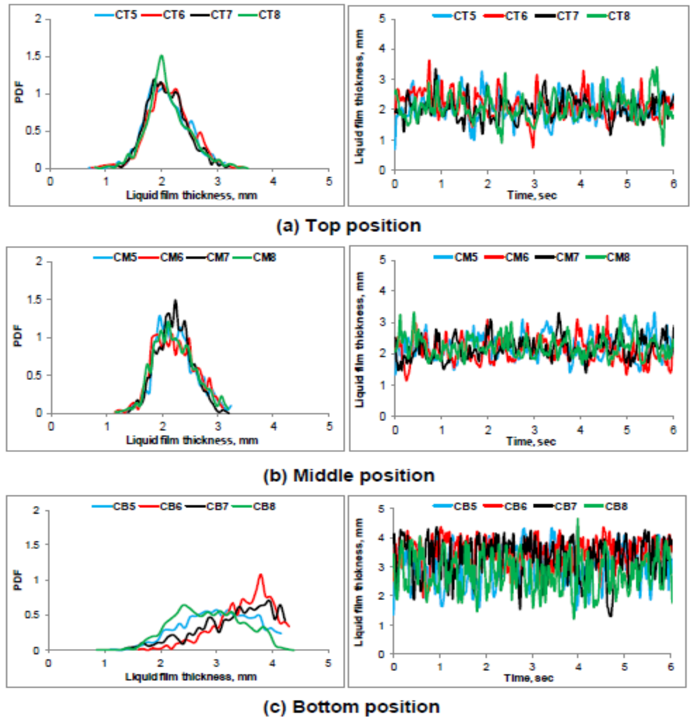

Figure 8 time profile & PDF of the water film at three positions in an upward section: (a) upper, (b) middle, and (c) lower, with water velocity=1 m/s and gas velocity= 2.67 m/s.

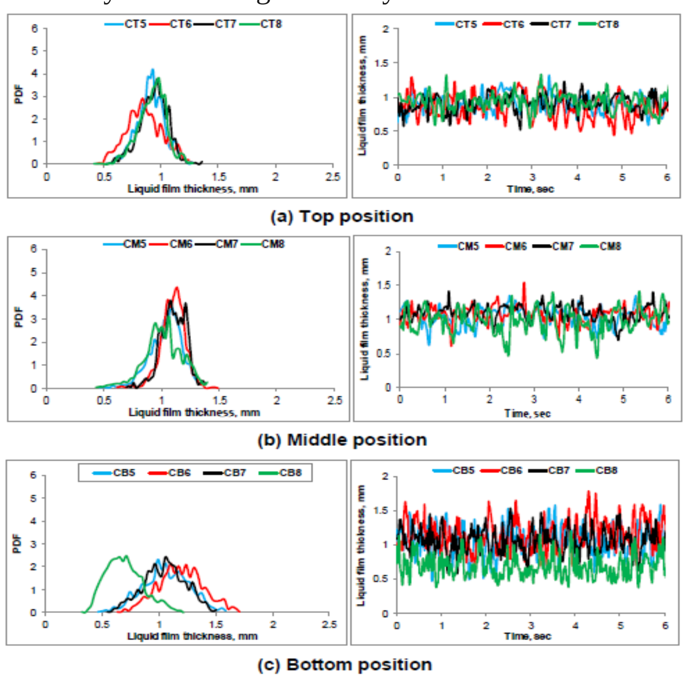

Figure 9 time profile & PDF of the water film at three positions in an upward section: (a) upper, (b) middle, and (c) lower, with water velocity=1 m/s and gas velocity= 18.56 m/s.

3.3 Frequency variance analyses of liquid film thickness

Frequency analyses were performed by PSD to show how a measured signal is distributed across various frequencies obtained from direct Fourier transformations. This method allows us to identify predominant frequencies in both descending and ascending sections for different air and water flow rates. The PSD shapes are distinct near bends but similar at locations farther away, even with the same flow rate (around five pipe diameters downstream from both bends).

3.3.1 Downward flow direction

Liquid film thickness frequencies (Fig. 10) reveal that at the top position, sensor T1 shows a significantly higher PSD height than those located apart at water and gas velocities equal to 0.1 m/s and 3.02 m/s, respectively. The PSD shapes indicate a reduction in PSD with increasing gas velocity. At gas velocity=12.47 m/s and water velocity=0.1 m/s, all positions displayed a similar trend with minimal bend effects. A similar pattern was observed at an air velocity of 28.87 m/s, where increased velocities further reduced bend effects.

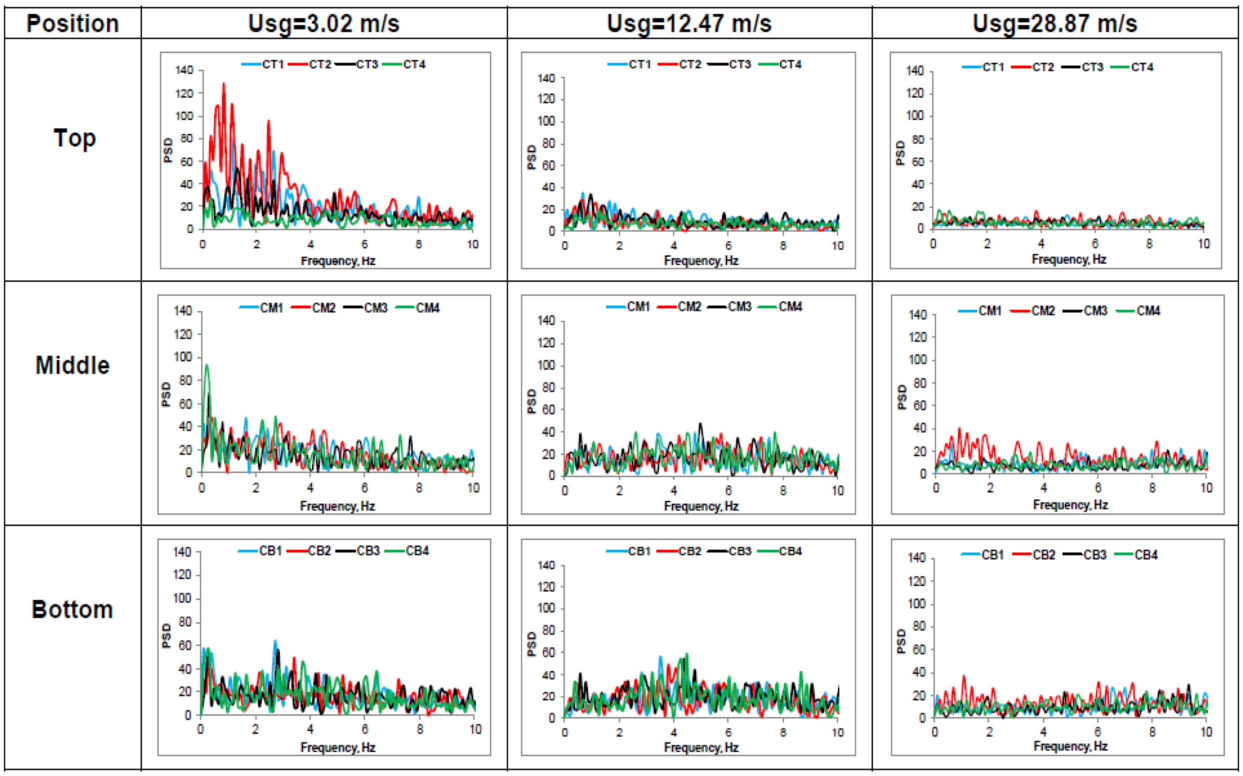

Figure 10 illustrates the PSD of water film at different heights—higher, middle, and lower positions-within the downflow, for various gas velocities, while maintaining a constant liquid velocity=0.1 m/s

In Fig. 11, with gas velocity=2.86 m/s and liquid velocity=0.48 m/s, the power spectral density (PSD) from the top location differs from that of the lower positions. When the gas velocity increases to a higher value (namely to 11.16 m/s), the PSD variation decreases, resulting in a nearly uniform frequency distribution at the mid-level and lower regions across all tested flow rates. This uniformity arises as the bending effect diminishes and the flow becomes fully developed. Notably, sensor T2 at the top shows higher PSD values at lower frequencies compared to T1, T3, and T4. The PSD plots remain consistent across all positions at the highest flow rate (at gas velocity=22.87 m/s), suggesting that flow distribution is stable in the downward section and less sensitive to increases in air flow rates.

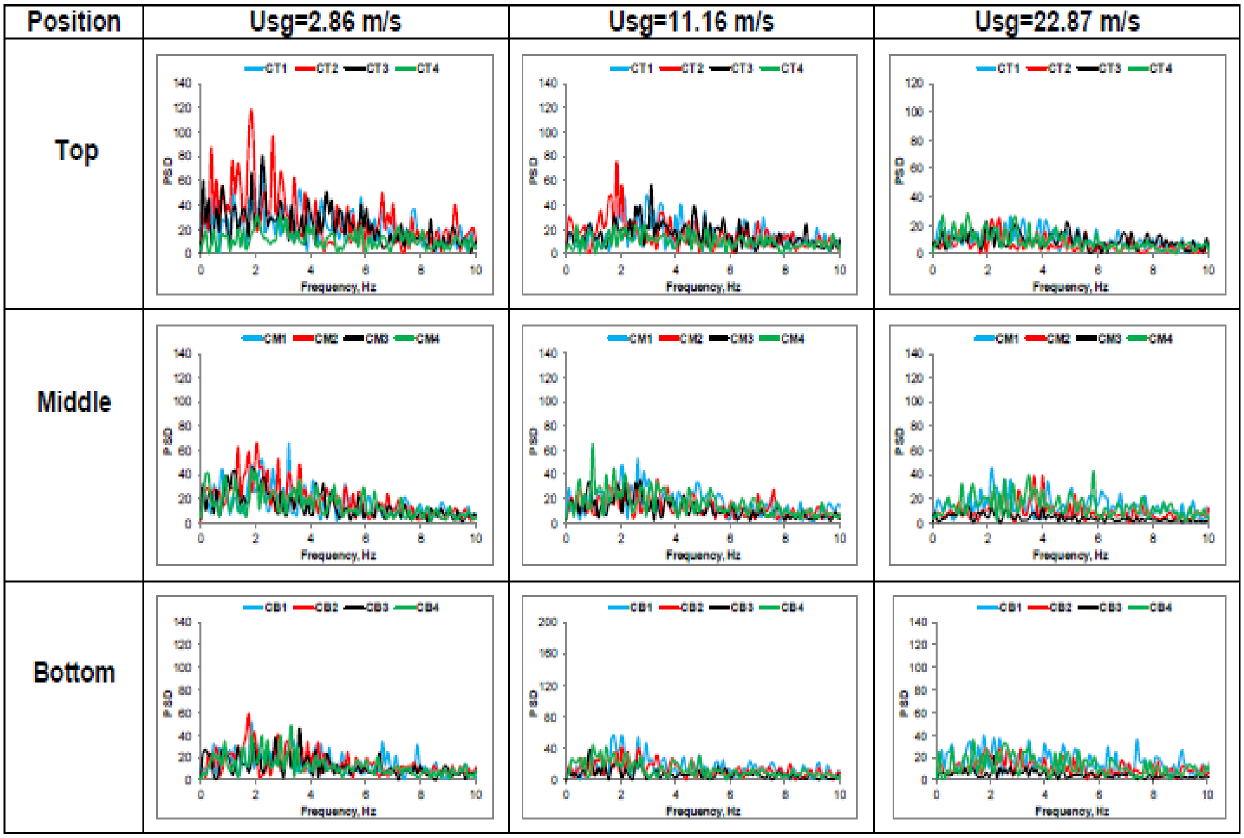

Figure 11 shows the power spectral density (PSD) of the liquid film at different locations of the downflow section, influenced by changes in the gas velocity and keeping the liquid velocity at 0.48 m/s.

Fig. 12 depicts the three positions of the PSD in the downward section at a constant liquid velocity=1m/s where the gas velocities are 2.67, 9.65, and 18.56 m/s. As the air superficial velocity increases, the PSD height decreases, reaching its minimum at 18.56 m/s. In the upper region, the PSD values differ significantly from the mid-level and lower regions. The middle and bottom PSD shapes are similar, indicating less bending and better flow development. At 2.86 m/s, the top position shows a higher PSD peak, with lower peaks at the middle and bottom. This trend persists at 9.65 m/s, while at 18.56 m/s, the PSD shapes become uniform.

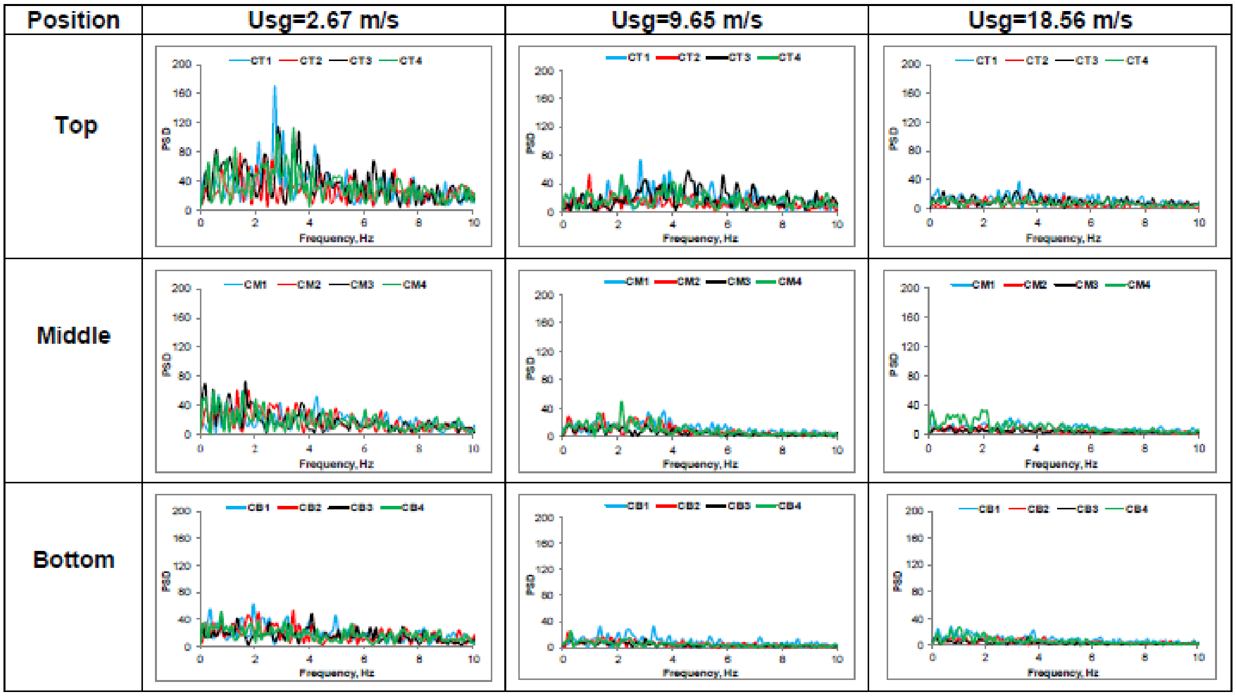

Figure 12 shows the power spectral density (PSD) of the liquid film at different locations of the downflow section, influenced by changes in the gas velocity and keeping the liquid velocity at 1 m/s.

3.3.2 Upward flow direction

The spectral evolution of the water film at various regions in the flow orientation is shown in Figs 13, 14, and 15, using Power Spectral Density (PSD) for various liquid and gas velocities. A clear trend emerges in all plots: as water's superficial velocity increases, the frequency increases as well. Higher water superficial velocities lead to a greater PSD amplitude compared to lower velocities, regardless of air velocities. Conversely, when water velocity is constant and air velocity increases, PSD amplitude decreases. In Fig. 13, the PSD frequency distribution remains consistent at air velocities of 3.02 m/s & 12.47 m/s across different positions. However, at the relatively high velocity of gas, differences in PSD amplitude and frequency location become noticeable, especially in the bottom position. This change indicates a transition from intermittent to annular flow, while lower air velocities show consistent intermittent flow results.

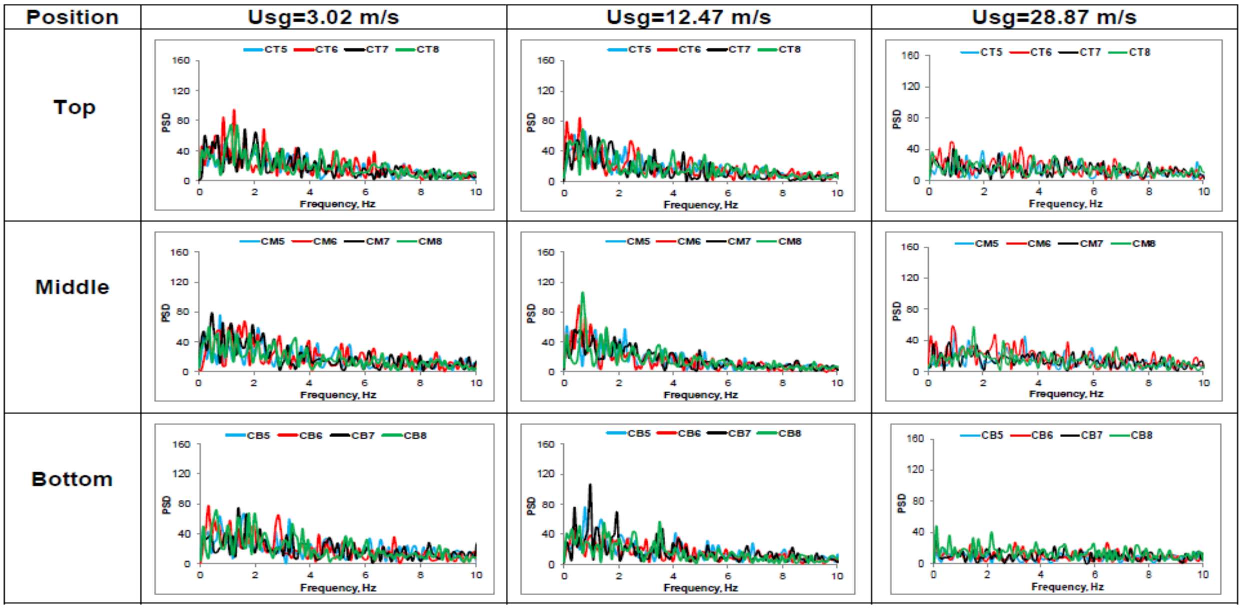

Figure 13 illustrates the PSD of water film at different heights—higher, middle, and lower positions—within the upflow, for various gas velocities, while maintaining a constant liquid velocity=0.1 m/s.

In Fig. 14, the water velocity was set to 0.48 m/s while the air velocities were set to 2.86, 11.16, and 22.87 m/s. It was observed that the PSD amplitude decreases with the increasing air velocities. The lower position has stronger PSD values and different dominant frequency locations for lower ranges of the air velocity 2.86 m/s and 11.16 m/s compared to higher positions. Yet, at the air velocity of 22.87 m/s, the PSD stopped being sensitive to the air positions and all positions were similar to each other, this highlights its sensitivity to the interaction of air and water velocities. Fig. 15 indicates that at greater airflow values, the spectral range amplitude is reduced and lowered.

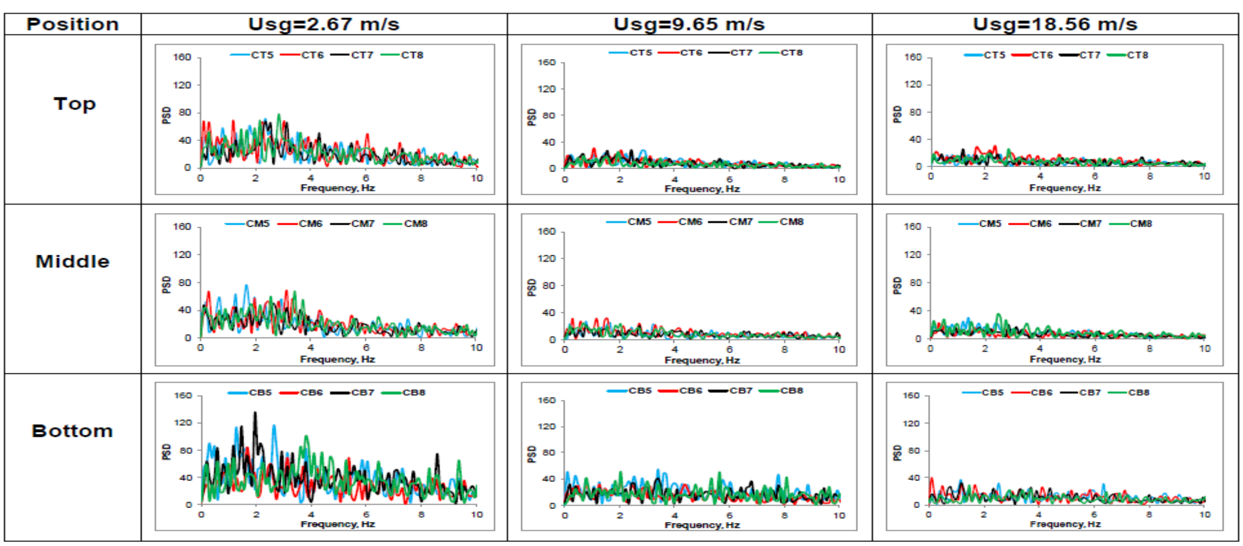

At air velocities of 2.67 and 9.65 m/s with water flowing at 1 m/s, the characteristics of frequency on the upper and middle areas are comparable, the lower position has somewhat higher PSD values. When air velocities were 18.56 m/s, the

PSD shapes were similar for all positions.

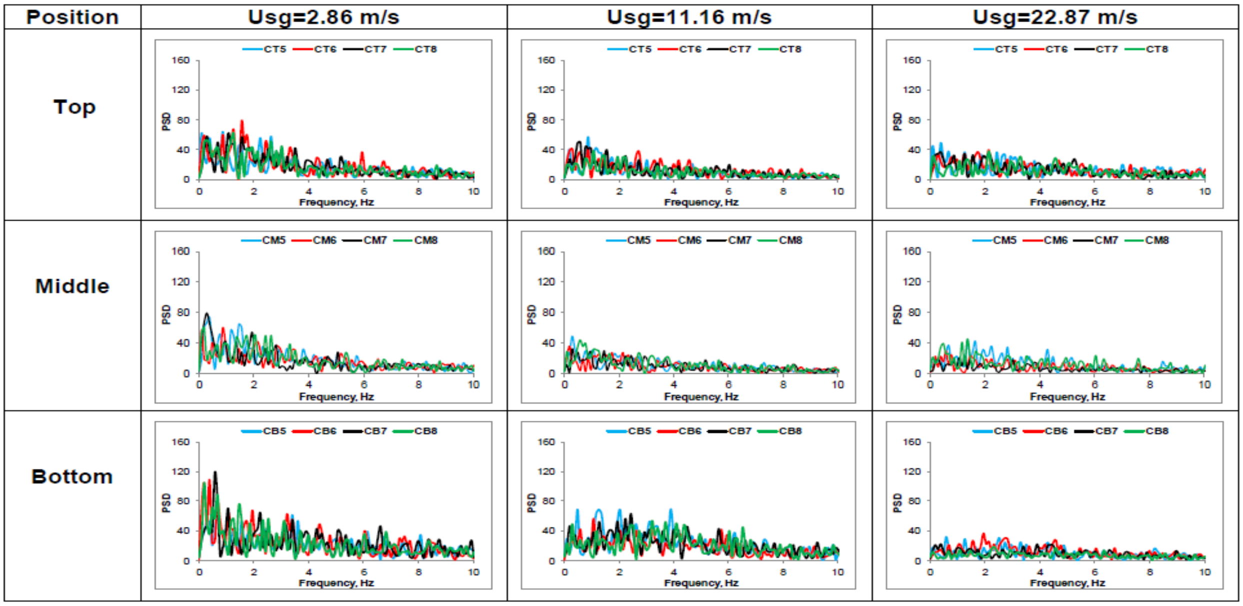

Figures 14 &15 illustrate the PSD of water film at different heights—higher, middle, and lower positions—within the upflow, for various gas velocities, while maintaining a constant liquid velocities=0.48 m/s &1 m/s, respectively.

4 Conclusion

The analysis of water film at various locations at the downflow path revealed that steep waves recorded by sensors T2 and M2 located at the top and middle film probes act as huge (disturbance) waves, particularly under low liquid and high gas flow rates. In comparison, sensors T1, T3, and T4 at the upper film device show shorter wavelengths and lower amplitudes, while sensors M1, M3, and M4 at the mid-level device exhibit reduced wavelengths and amplitudes relative to M2. In different flow conditions, such as very low and very high air and water flow rates, recordings from the middle and bottom probes align due to the stabilization of the liquid film. Additionally, PSD shapes near the bend (five pipe diameters downstream from the upper curvature) differ considerably from those positioned farther downstream. The analysis indicates that both air and water superficial velocities significantly impact flow dynamics in an upward orientation. As water superficial velocity increases irrespective of air flow velocity the PSD frequency rises. Conversely, with constant water flow and increasing air velocity, the amplitude of the PSD decreases.

References

Smith, J., Johnson, R., & Williams, A. (2010). Experimental investigation of fluid dynamics and heat transfer in serpentine pipes. *Journal of Engineering Research*, *15*(3), 112-125.

Wang, Y., Li, H., & Zhang, J. (2012). Measuring liquid film thickness in vertical upward pipes using electrical capacitance tomography. *Flow Measurement and Instrumentation*, *28*, 53-60.

Smith, A., Johnson, B., & Williams, C. (2015). Utilizing laser-induced fluorescence to measure liquid film thickness in a serpentine microchannel under varying flow conditions. *Microfluidics and Nanofluidics*, *19*(5), 1123-1135.

Chen, X., Zhang, L., & Wang, Q. (2015). Experimental study on the influence of surface tension on liquid film thickness in serpentine pipes. *Experimental Thermal and Fluid Science*, *67*, 170-179.

Choi, S., Kim, J., & Lee, C. (2015). Comparative analysis of optical measurement techniques for quantifying liquid film thickness in vertical upward pipes. *Measurement Science and Technology*, *26*(6), 065303.

Wang, J., Liu, Q., & Zhang, Y. (2016). Investigating the interplay between flow regimes and liquid film thickness and examining the occurrence of flow instabilities in serpentine pipes. *Journal of Fluids Engineering*, *138*(7), 071302.

Zhang, H., Li, W., & Wang, L. (2017). Employing gamma-ray densitometry to measure liquid film thickness in vertical downward pipes. *Nuclear Instruments and Methods in Physics Research Section A: Accelerators, Spectrometers, Detectors and Associated Equipment*, *854*, 11-19.

Lee, J., Park, S., & Kim, H. (2017). Strategies for enhancing heat transfer efficiency in serpentine heat exchangers by optimizing liquid film thickness. *International Journal of Heat and Mass Transfer*, *108*, 195-205.

Park, K., Kim, M., & Lee, S. (2017). Characterizing liquid film thickness in vertical pipes using electrical impedance tomography, X-ray tomography, and laser-based methods. *Measurement Science and Technology*, *28*(8), 085301.

Smith, A., Johnson, B., & Williams, C. (2018). Comparative analysis of liquid film measurement techniques in upward and downward flow configurations: Ultrasonic sensors, capacitance probes, and optical methods. *Experimental Thermal and Fluid Science*, *94*, 60-71.

Liu, Y., Wang, Q., & Zhang, H. (2019). Experimental characterization of liquid film dynamics in vertical downward pipes prone to gas entrainment. *Chemical Engineering Science*, *206*, 47-58.